An experimental study on the rehabilitation performance of CFRP-strengthened bubble deck slabs: effects of void size and preloading levels

Muntadher Ragheef Bader, Abdulkhalik J. Abdulridha
Department of Civil Engineering, College of Engineering, Al-Nahrain University, Jadriya, Baghdad, Iraq
montader.mciv22@ced.nahrainuniv.edu.iq
abdulkhalik.j.abdulridha@nahrainuniv.edu.iq

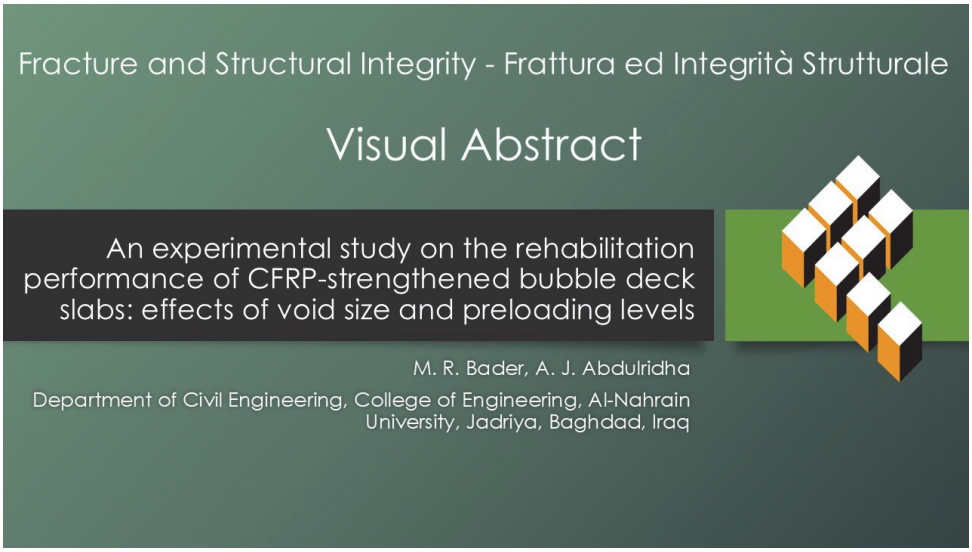

OPEN ACCESS

Citation: Bader, M. R., Abdulridha, A. J., An experimental study on the rehabilitation performance of CFRP-strengthened bubble deck slabs: effects of void size and preloading levels, Fracture and Structural Integrity, 74 (2025) 115-128.

Received: 28.07.2025
Accepted: 16.08.2025
Published: 16.08.2025
Issue: 10.2025

KEYWORDS. Rehabilitation, Damaged, Two-way slab, CFRP sheets, Bubbled slab

INTRODUCTION

Reinforced concrete (RC) slabs are the fundamental structural component of infrastructure, bridges, and structures. To eliminate the dead weight of the concrete construction while maintaining its structural integrity, the bubble deck slab has undertaken its role as an environmentally friendly and lightweight structure. The concrete volume is significantly reduced in these slabs due to using porous plastic spheres in the slab core. Consequently, there is a reduction in self-weight and material. Despite the environmental and economic advantages of bubble deck slabs, the strength of striking shear and the rehabilitation of such slabs after they are damaged are the primary challenges they present. The problem is particularly severe in two-way slabs, where the load can transmit more intricately and local degradation induces early collapse. Therefore, it is imperative to identify the methods of strengthening that can be employed to enhance or restore the load-bearing capacity of bubble deck slabs that have been damaged. The high strength-to-weight ratio, corrosion resistance, and ease of installation of Fiber Reinforced Polymer (FRP) systems, particularly the Carbon Fiber Reinforced

Polymer (CFRP) sheets, have typically garnered significant attention. Several researchers have demonstrated the efficacy of CFRP in reinforcing the conventional RC surface. Nevertheless, there is a dearth of research on bubble deck systems, particularly about the extent of devastation and the diverse sizes of voids. The present paper focuses on the externally bonded CFRP ligatures used to repair the two-way bubble slab with plastic spheres (50- and 60-mm in diameter). It evaluates the ultimate strength, fracture pattern, deflection behavior, and flexural behavior of such slabs before and after retrofitting. The structural efficiency and practical application of CFRP retrofitting of lightweight RC systems are illuminated by comparing the rehabilitated specimens to the control solid material in this study [1-5].

As a result of their high strength-to-weight ratio, corrosion resistance, and simplicity of installation, Fiber Reinforced Polymer (FRP) systems, particularly (CFRP) sheets, have garnered widespread recognition. In numerous studies, CFRP effectively strengthens conventional reinforced concrete slabs and columns [6]. Nevertheless, research is scarce on applying this technology to innovative slab systems, such as bubble decks, with a particular emphasis on the significance of pre-damage levels and cavity size. Some recent research has begun to investigate the structural behavior of voided and lightweight slabs, emphasizing their distinctive response to loading and repair. The structural performance of layered hollow-core slabs was examined by Ghamry et al. (2022) [2], who underscored the necessity of customized reinforcing solutions for the altered stress distribution and reduced concrete cross-section. A study by Ismael et al. (2025) [7] examined voided ferrocement slabs with fibrous concrete. The results indicated that the ductility was enhanced, but the slabs were also more susceptible to flexural fracture factors. Consequently, effective rehabilitation strategies are required. Khadim and Abdulridha (2024) [8] investigated the behavior of pre-cracked lightweight concrete slabs in FRP retrofitting. They discovered that CFRP application substantially restored load capacity, although efficiency decreased with more severe initial damage. Similarly, Aborgheef and Abdulridha (2025) [9] have shown that CFRP sheets can effectively repair damaged corbels. The performance of these sheets is significantly influenced by the preloading level and bonding quality findings, which are directly pertinent to bubble deck applications where interfacial integrity is important. There is currently no study that has systematically assessed the rehabilitation of two-way bubble deck slabs using CFRP while varying both the vacuum diameter and the severity of pre-damage, despite these advancements. Bubble decks are being utilized in sustainable construction at an increasing rate; however, their repair under service-induced damage remains a practical challenge. This discrepancy is substantial. The current investigation addresses this requirement by conducting an experimental evaluation of the efficacy of externally bonded CFRP sheets in restoring the structural performance of bubble deck slabs with 50 mm and 60 mm cavities, which were subjected to varying preloading levels. This study uses externally bonded CFRP sheets to rehabilitate two-way bubble deck slabs with voids of 50 mm and 60 mm diameter. The flexural behavior, cracking patterns, deflection response, and ultimate strength of the slabs are evaluated before and after retrofitting. The results are compared to a solid control slab to evaluate the structural efficiency and practical usability of CFRP strengthening in lightweight RC systems.

TWO-WAY BUBBLED SLABS

Bubble slabs are innovative structural systems that utilize cavities within concrete slabs to reduce dead load without compromising structural integrity or load-bearing capacity. The bubbles are subsequently shaped to the appropriate shape, which is typically achieved by molding them from plastic or foam material. A grid pattern is then established throughout the structure. The outcome will resemble a 3D system of interconnected spheres. This specifically addresses the quantity of concrete consumed; consequently, the outcome is a platform that is lighter in weight but retains the same strength and rigidity characteristics as conventional solid slabs, as illustrated in Fig. 1. Bubble panels can transfer loads in both directions more effectively than traditional panels due to their ability to transfer loads through multiple voids. This is achieved through a balanced resistance to pressure and enhanced direct force interference. The entire slab is endowed with inherent flexibility due to the void configuration in a grid pattern, which ensures that the slab remains upright and unharmed in the event of localized damage or slab failure. The bubble slab load is further reduced in both directions by voids, corresponding to the dead load coefficient of slabs of identical thickness. Dead load redistribution offers several benefits, including the potential for a lightweight superstructure and reduced foundation requirements. Furthermore, it enables the construction industry to create more environmentally favorable construction technologies to prevent environmental contamination during extraction, transportation, and construction processes. Two-way bubble panels offer superior thermal insulation, which is further enhanced by the presence of cavities within the structure. The air trapped in the voids serves as a barrier, prohibiting heat transmission into the slab. Consequently, the building's energy consumption for cooling or heating can be reduced. Applying modularity to two-way bubble sheet systems contributes to increased construction efficiency and facilitates on-site work while providing significant speed. Projects with urgent deadlines can implement this approach, as it will substantially decrease costs and enhance project scheduling [10-13].

REHABILITATION OF STRUCTURAL MEMBERS

The two-way bubble slab mending procedure aims to enhance the functionality, durability, and structural integrity of the current bubble slab systems. Step one of the rehabilitation processes involves conducting a comprehensive structural assessment of two-way bubble slabs to ascertain the current condition of the slabs. This survey procedure may involve various techniques, including non-destructive testing, simple visual inspections, or structural analysis, to identify the components of the structure that are susceptible to damage, structural weakening, or deterioration. Initially, it is imperative to determine the type and extent of the injury that has been created. Consequently, this will establish the most suitable approach. Methods such as repairs and enhancements that address these deficiencies can be implemented during the structural assessment. Concrete repair, corrosion protection, the design of reinforced bars in the roof foundation, additional support structures, and numerous other methods may be implemented. The selection of repair and fortifying methods is contingent upon the specific circumstances of the repair, the slab's requirements, and the performance of the repaired slab, regardless of whether it is a trench or a slab. Additionally, the recoloring and enhancement of the durability factor may be implemented to ensure that the two-way bubble slabs continue to function for extended periods and address the deficiencies. This could be accomplished by employing waterproofing systems, corrosion inhibitors, or surface coatings to prevent degradation mechanisms, including rust corrosion, alkali-aggregate reaction, and freeze-thaw cycles. It is imperative to determine the economic benefits of alternative rehabilitation activities and make informed decisions regarding allocating resources and attaining performance objectives. It is important to note that recovery efforts may be beneficial if they incorporate sustainability elements and reduce environmental impact while promoting resource use [14-19].

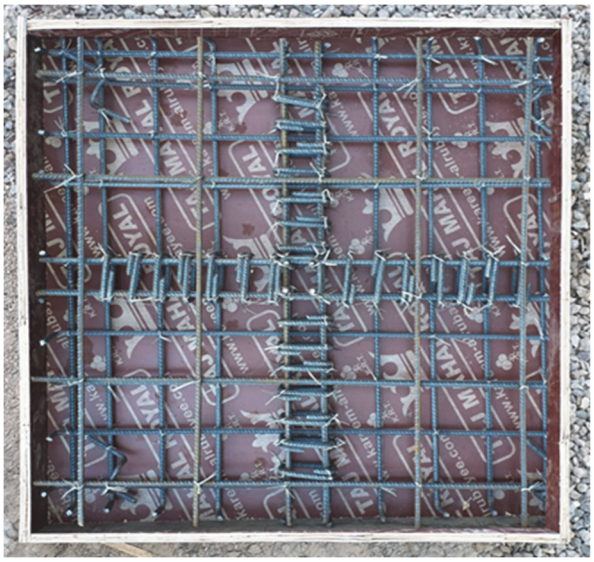

Figure 1: Mold of slab.

OUTLINE OF THE EXPERIMENTAL SECTION

The experimental program included nine 1000 mm × 1000 mm × 125 mm bubble reinforced concrete slab specimens. One of these specimens was designated the solid control slab (SS-Control); the other eight specimens were bubble slabs. A cylindrical object, a plastic sphere with diameters of 50 and 60 mm, was embedded in a regular grid pattern at the center of the slab thickness. The slabs were reinforced on both sides with upper and lower steel lattices to illustrate slab movement in two directions. In order to guarantee two-way load transmission, steel mesh was applied to both the top and bottom faces of all slab specimens. 10 bars of 10 mm diameter, spaced at 100 mm center-to-center in each direction, comprise the bottom (tension) stratum (10 bars per direction). The top (compression) layer comprises four bars with a diameter of 10 mm, which are positioned 250 mm center-to-center in each direction. The primary purposes of this layer are to regulate temperature and contraction. The effects of vacancy size and CFRP rehabilitation were isolated by maintaining a consistent total steel area across all specimens, as illustrated in Fig. 1. The reinforcement's yield strength, as determined by tensile testing by ASTM A1064 (2022) [20], was 460 MPa. Each monolith was cast with a central column butt (100 mm

× 100 mm) to enable punch shear simulation. The severity of preload injury prior to CFRP rehabilitation was used to identify bubble slab groups, as illustrated in Tab. 1. The concrete required a compressive strength of 30 MPa, even though ready-mix concrete was employed to cast all panels. The reinforcing rods exhibited a tensile yield strength of 460 MPa. The reinforcing bars were subjected to tensile testing by ASTM A1064, while standard cylindrical tests were conducted by ASTM C39 (2024) [21]. The bidirectional carbon fiber-reinforced plastic (CFRP) layers integrated into the rehabilitation works had a modulus of elasticity of 230 GPa, a thickness of 0.167 mm, and a tensile strength of approximately 3500 MPa. They were affixed using an epoxy bonding system based on ACI 440.2R (2017) [22]. Subsequently, specimens SB-5-50, SB-5-60, SB-5-75, SB-6-50, SB-6-60, and SB-6-75 were cured and preloaded to 50%, 60%, and 75% of their previously measured maximal capacity, as determined by the SB-5-0 and SB-6-0 tests. The CFRP sheets were reattached in the orthogonal directions after the rear of each damaged specimen was rehabilitated following unloading.

Specimen designation	Description
SS-Control	Referential Specimen without Bubbled and without CFRP
SB-5-0	Bubbled slab with 50 mm void diameter without damaged and without CFRP sheets
SB-5-50	Bubbled slab with 50 mm void diameter with 50% damaged repairing with CFRP sheets
SB-5-60	Bubbled slab with 50 mm void diameter with 60% damaged repairing with CFRP sheets
SB-5-75	Bubbled slab with 50 mm void diameter with 75% damaged repairing with CFRP sheets
SB-6-0	Bubbled slab with 60 mm void diameter without damaged and without CFRP sheets
SB-6-50	Bubbled slab with 60 mm void diameter with 50% damaged repairing with CFRP sheets
SB-6-60	Bubbled slab with 60 mm void diameter with 60% damaged repairing with CFRP sheets
SB-6-75	Bubbled slab with 60 mm void diameter with 75% damaged repairing with CFRP sheets

Table 1: Corbel specimens' descriptions.

Figure 2: Schematic illustration of the experimental test setup.

The formworks were constructed from 15 mm flat plywood and utilized for concrete casting. The forms have a thickness of 125 mm and dimensions of 1000 x 1000 mm. The materials (cement, gravel, and sand) were weighed and packaged; refer to Fig. 2. The steel bar reinforcements were subsequently inserted after the interior faces of the formwork were lubricated. A steel rod manually vibrated the concrete mix, and the form's exterior faces were hammered with a rubber hammer after the concrete was cast inside the form. A manual trowel was employed to level and smooth the concrete surface. After washing and lubricating the forms, three cubes of the dimensions (150x150x150) mm are cast in steel cube molds during concrete casting. After one day of casting, the cubes were demolded and subjected to the same conditions as the samples. Fig. 3 illustrates that concrete curing commenced one day after casting, with a moist canvas utilized for 28 days. A universal testing equipment with a maximum capacity of 200 tons was employed to test all slab specimens under monotonic central loading. The slabs were supported along their four edges, which simulated bidirectional deformation. The slab is four-edge simply supported on rollers, with a central column stub (100 mm × 100 mm). Load is applied through a 100 mm × 100 mm steel plate aligned with the column. LVDTs are positioned at midspan and supports to measure vertical deflection, as shown in Fig. 4. Failure modes were also precisely identified using crack patterns and ultimate failure mechanisms (i.e., flexural, punch shear, or mixed shear and flexural failure). The observations of the reconstituted CFRP slabs were similar, and the performance of the reinforcement work was also observed in terms of crack reduction and increased stiffness.

Figure 3: Casting of slabs.

Figure 4: Test set-up.

TESTING SETUP AND LOADING PROTOCOL

All specimens were subjected to monotonic central loading with four-edge supported conditions to simulate two-way flexural behavior. The burden was uniformly transferred by placing a rigid steel loading plate (100 mm × 100 mm) at the center of the slab, directly above the cast-in column stub. The support system comprised steel rollers to prevent restraining moments and facilitate unfettered rotation. Three linear variable differential transformers (LVDTs) were employed to measure deflections: one at midspan and two at opposite supports. An automated data acquisition system was employed to record data perpetually. Loading was performed in a universal testing machine with a capacity of 200 tons, with displacement control. The initial loading rate was 0.5 kN/min to capture the first cracking and elastic behavior precisely. A controlled failure was achieved by increasing the rate to 1.0 kN/min after considerable cracking was developed, typically beyond 40% of the ultimate load. This protocol guaranteed that the test conditions were consistent and reproducible for all specimens.

SELECTION OF PRELOADING LEVELS

The preloading levels of 50%, 60%, and 75% of the ultimate load were chosen to simulate realistic damage scenarios in service-aged structures ranging from early-stage fracture to near-failure conditions. These thresholds are consistent with the typical service load levels (40–60% of capacity) and reflect the progressive stages of stiffness degradation and fracture development observed in reinforced concrete slabs. The practical upper limit for effective CFRP rehabilitation is 75%, beyond which bond integrity and concrete cohesion may be compromised. This choice is substantiated by prior research on FRP-strengthened members [6-9] and verified by preliminary testing, which showed that specimens preloaded to 75% maintained adequate structural integrity for retrofitting while evidencing substantial damage.

CFRP APPLICATION AND BONDING PROCEDURE

The carbon fiber-reinforced polymer (CFRP) sheets used for strengthening were bidirectional (0°/90°) with a nominal thickness of 0.167 mm, tensile strength of 3,500 MPa, and elastic modulus of 230 GPa (SikaWrap®-301/302 Biaxial Grid). The sheets were bonded using a two-step epoxy system in accordance with ACI 440.2R-17 guidelines for externally bonded FRP systems:

- Primer: SikaDur®-31 CF Rapid (two-component epoxy primer, mix ratio 3:1 by weight).
- Adhesive: SikaDur®-330 (high-strength, thixotropic epoxy adhesive, mix ratio 4:1 by weight).

The concrete surface (tension face) was prepared by ASTM D7234 (2021) [23] before primer application to guarantee an appropriate surface profile for bond strength. The laitance was removed from the surface by grinding it with a diamond cup

wheel, resulting in a surface roughness (Rz) of approximately 0.85 mm. This was confirmed using a replica putty technique. The substrate was cleansed with isopropyl alcohol and compressed air to eliminate contaminants and dust. The primer was uniformly applied and permitted to cure for 2 hours (induction period) in ambient conditions. The adhesive was applied with a 3 mm notched trowel to guarantee a uniform thickness. The CFRP sheet was meticulously positioned to prevent wrinkling, rolled with a resin roller to eradicate air voids, and smoothed from the center outward. The average temperature was 22 ± 2°C, and the relative humidity was 50 ± 5%. All specimens were cured for 7 days in ambient laboratory conditions. These conditions follow the manufacturer's specifications for SikaDur®-330 and the standard curing practices for epoxy-based FRP systems as outlined in ACI 440.2R (2017) [22]. The specimens were visually inspected for delamination, air pockets, or edge debonding after curing, before re-testing.

RESULTS AND DISCUSSIONS

The SS-Control module was tested to establish a benchmark for comparing the structural performance of bubble slabs. In the void-free slab, a flexural pattern developed up to an ultimate load of 183.6 kN, a mid-span deflection of 17.6 mm, and failure occurred due to tension cracking at the top and collapse at the bottom. ACI 318 specifies that the service deflection should not exceed L/240, i.e., 4.17 mm for a 1000 mm span beam. Although the actual deflection exceeded the allowable limit, this result did not reflect the conditions the structure would encounter in use. We used the SS-Control module as a reference point for analyzing reconstructed bubble slabs, as shown in Figs. 5 and 6.

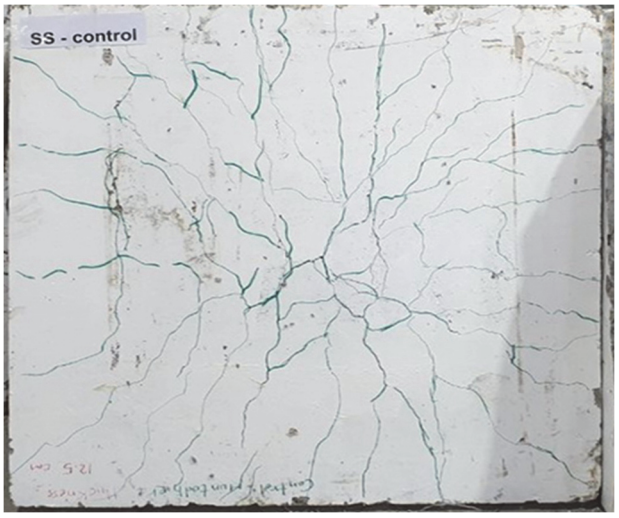

Figure 5: Crack pattern of the solid slab.

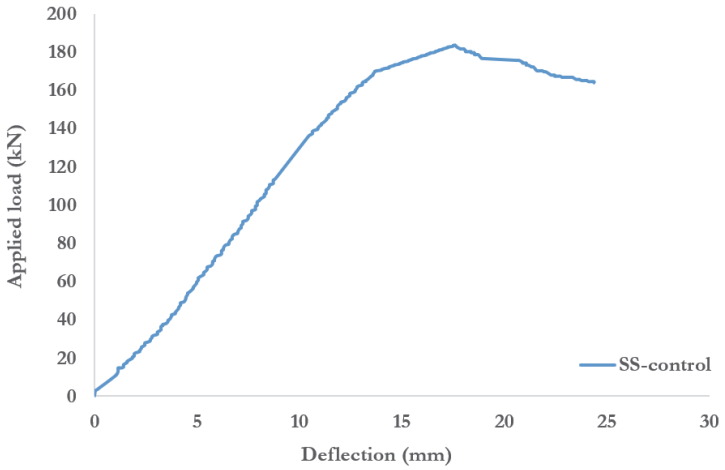

Figure 6: Load-deflection curve of solid slab.

BEHAVIOR OF BUBBLED SLAB WITH 50 MM DIAMETER (GROUP 1)

Bubble slabs with voids measuring 50 mm in diameter comprised group 1. The mid-span movement of the unreinforced bubble slab in this group was slightly greater, even though its load-bearing capacity was slightly lower. This suggests that the slab's rigidity has reduced. All reconstructed specimens (with pre-damage rates of 50%, 60%, and 75%) exhibited a stronger or improved structural response following reinforcement with carbon fiber-reinforced plastic (CFRP). The ultimate burden increased by 1% to 4% following the replacement, contingent upon the severity of the damage that existed prior to the completion of construction. The reinforced specimens exhibited a deflection at failure up to 23% lower than the unreinforced bubble slab, exhibiting superior rigidity. Tab. 2 and Figs. 7-9 demonstrate that Group 1 exhibited a positive response to CFRP rehabilitation and a mixed flexural and debonding behavior that persisted or stabilized at higher levels of damage. Plastic cavities with a diameter of 50 mm were present in each slab of Group 1. The failure mode of the specimen (SB-5-0) was characterized by bottom fractures that developed in the center and progressed toward the edges. The failure pattern was flexural and debonding.

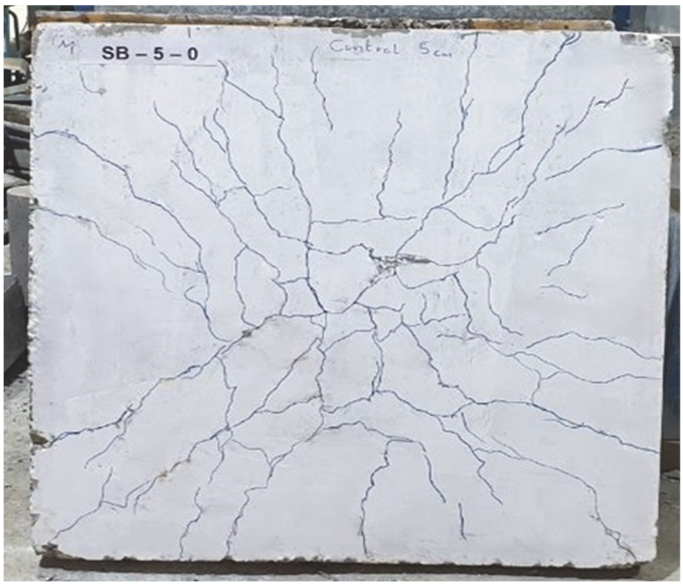

Figure 7: Crack pattern of slab specimen SB-5-0.

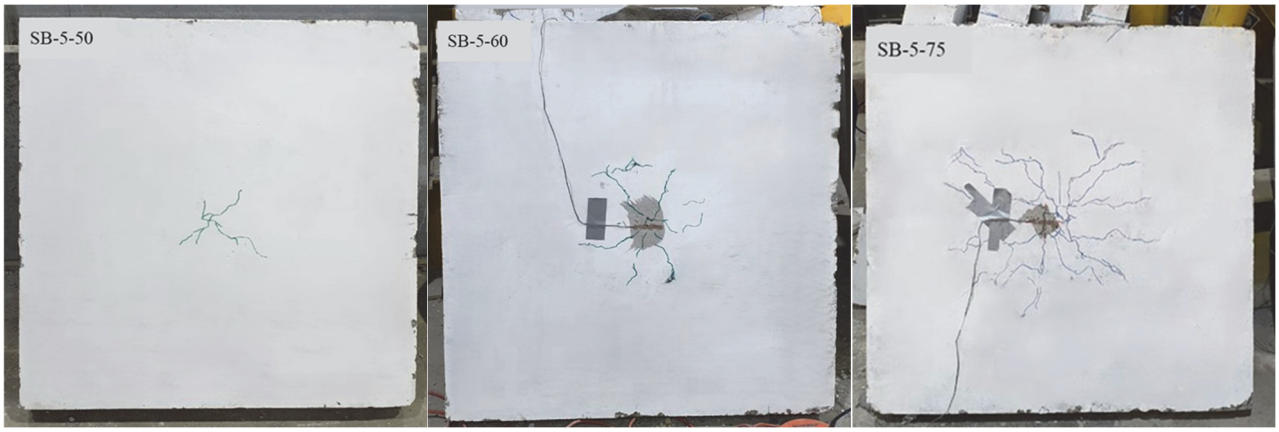

Figure 8: Crack patterns in 50 mm void bubble slabs before CFRP rehabilitation and re-testing to failure: (a) SB-5-50, (b) SB-5-60, (c) SB-5-75.

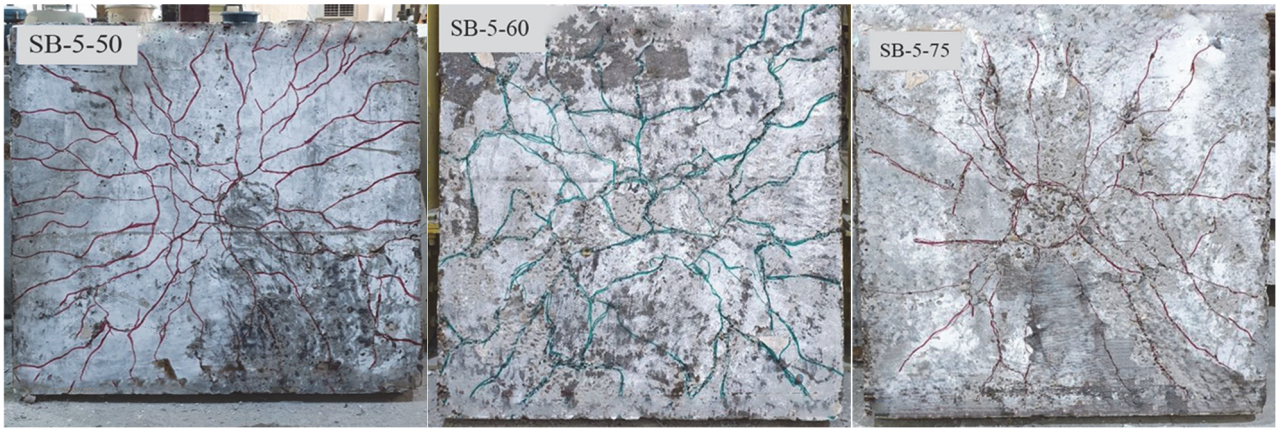

Figure 9: Crack patterns in 50 mm void bubble slabs after CFRP rehabilitation and re-testing to failure: (a) SB-5-50, (b) SB-5-60, (c) SB-5-75.

The fractures in the SB-5-50, SB-5-60, and SB-5-75 slabs became more compact and cohesive after the CFRP slabs were cured. The fractures were primarily situated in restricted areas and were not extensive; the same was true of the concrete crushing. The CFRP slabs significantly enhanced the rigidity and strength of the concrete structure during flexure. The maximal load increased by 1–4% compared to the performance of the unreinforced slab. The stiffness was enhanced, as evidenced by a 15–23% reduction in deflection at the maximum strain. The carbon fiber-reinforced plastic (CFRP) reinforcement is responsible for the enhanced energy dissipation and delayed failure mechanisms indicated by the crack patterns. Graphs and samples demonstrated that carbon fiber reinforced plastic (CFRP) sheets performed exceptionally well in the repair of microbubble tiles, despite significant pre-damage. Additionally, a mixed failure between flexure and bond separation was observed.

BEHAVIOR OF BUBBLED SLAB WITH 60 MM DIAMETER (GROUP 2)

Bubble slabs with voids measuring 60 mm in diameter comprised group 2. In the unreinforced specimen, the ultimate load was approximately 13% lower than the solid specimen's, even though its deflection was slightly higher. This may be attributed to the lower strength but similar failure toughness. The structural performance of all reconstructed specimens (loaded at 50%, 60%, and 75%) exhibited some or significant signs of recovery after the CFRP reinforcement was completed. Depending on the severity of pre-existing damage, the ultimate burden increased by 5 to 9% compared to the unreinforced slab. Adding layers reduced deflection, as evidenced by the substantial effect of preloading: slabs lacking preloading experienced deflection decreases of up to 20%. Group B responded favorably to CFRP rehabilitation; however, Group 2 recovered a lesser percentage of its original strength than Group 1 when the damage was more severe, as illustrated in Tab. 2 and Figs. 10, 11, and 12. As with all specimens, the predominant failure type for the Group 2 panels was a mixed flexural-delamination failure. The SB-6-0 specimen experienced the development of typical downward-curving fractures in the central region, which subsequently spread. The specimen's top bowed, and the concrete in that area fractured extensively, indicating a classic flexural failure. In the SB-6-50 specimen, the widest cracks were smaller and concentrated in a single location, suggesting that the CFRP laminates assisted in slowing the fracture process and making it more localized. The CFRP enabled controlled fissure growth and maintained failure stability, even though the fracture zone in the SB-6-60 was denser. The SB-6-75 failure was characterized by the partial detachment of the CFRP reinforcement layer and early cracking in the upper layer. The energy absorption and the bond between the fibers and the resin were substantially shorter, even though they were not yet considered a buckling failure. The toughened panels outperformed SB-6-0 regarding fracture size and growth at moderate damage. The post-cracking resilience of CFRP panels was enhanced due to delayed surface expansion and delamination. We observed a decrease in the reliability of damage recovery in the 60% to 75% damage range, which suggests that the CFRP panels are less effective and that the components are deteriorating more rapidly. This confirms that CFRP panel repair is more effective for moderate damage and that fissure control is crucial for optimal post-repair performance.

Specimen	Pre-damage Level	Strengthening	Ultimate Load (kN)	Change vs Control
SS-Control	-	Without	183.6	-
SB-5-0	-	Without	176.7	- 3.76%
SB-5-50	50 %	CFRP	180.9	- 1.47%
SB-5-60	60 %	CFRP	178.1	- 3.00%
SB-5-75	75 %	CFRP	173.0	- 5.77%
SB-6-0	-	Without	158.8	–13.5%
SB-6-50	50 %	CFRP	172.0	–6.3%
SB-6-60	60 %	CFRP	167.9	–8.5%
SB-6-75	75 %	CFRP	151.4	–17.5%

Table 2: Ultimate load capacity.

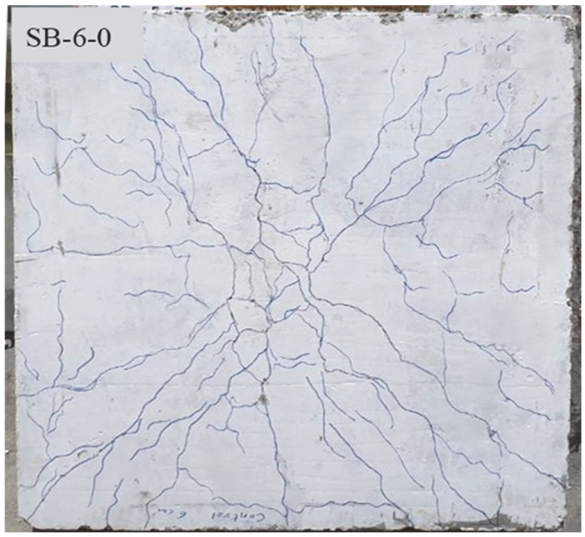

Figure 10: Crack pattern of slab specimen SB-6-0

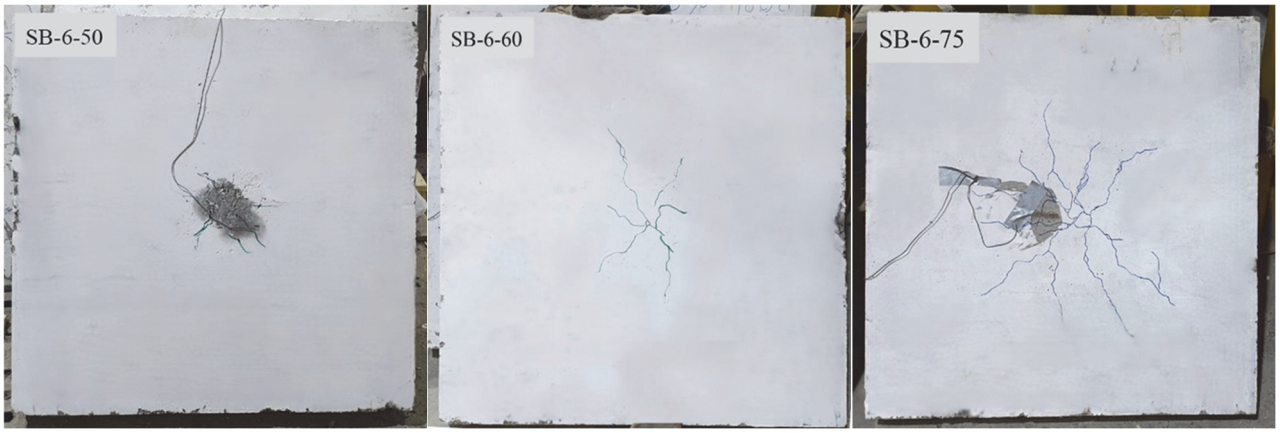

Figure 11: Crack patterns in 60 mm void bubble slabs before CFRP rehabilitation and re-testing to failure: (a) SB-6-50, (b) SB-6-60, (c) SB-6-75.

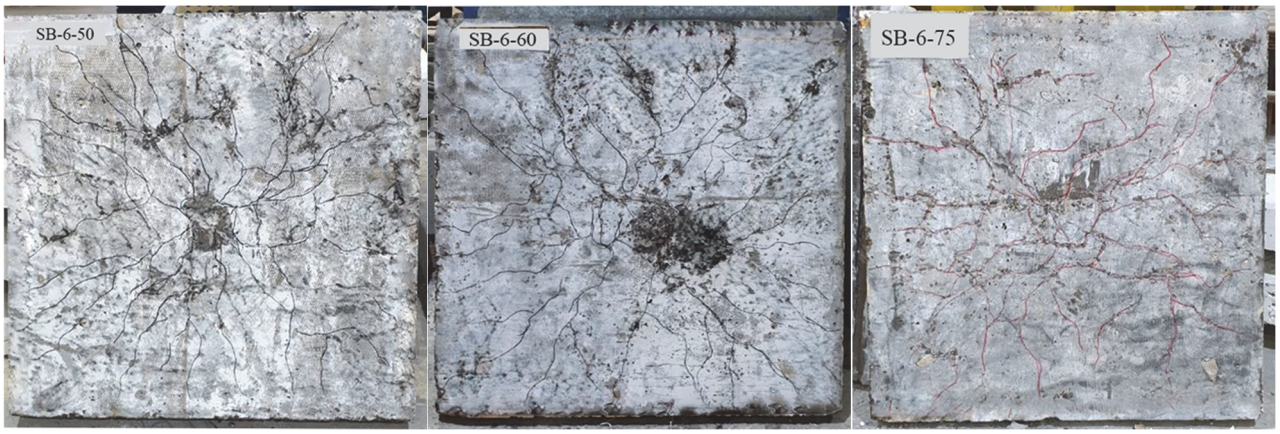

Figure 12: Crack patterns in 60 mm void bubble slabs after CFRP rehabilitation and re-testing to failure: (a) SB-6-50, (b) SB-6-60, (c) SB-6-75.

LOAD-DEFLECTION CURVES

In order to assess the effects of void confinement and carbon fiber reinforced polymer (CFRP) panel reinforcement, the behavior of Group 1 panels (50 mm void diameter) was compared to that of a rigid control panel. The primary reference points for comparison were the maximal stress and deflection of the SS-Control panel. Compared to the panel, the SB-5-0 experienced a slight failure at approximately 95.9% of the panel stress. However, it began to deform and become less stiff at approximately 9.1% earlier. The SB-5-50 bar recovered more effectively after being reinforced with CFRP panels, attaining approximately 98.5% of its control and reducing deflection by approximately 22.5%.
In comparison to the SS-Control panel, the SB-5-60 recovered nearly all of its load and experienced a deflection reduction of over 10% during deflection. The structure was firmer after the damage had increased prior to repair, as it responded to the load by approximately 94.3% and reduced deflection by approximately 25.5%. The results demonstrate that the load-bearing capacity is significantly enhanced by adding carbon fiber-reinforced plastic (CFRP), which also enhances the stiffness of slabs marginally weakened before the repair. The reliability of flexural recovery is further confirmed by the fact that the behavior of the reinforced slabs approaches that of the solid model as the strength increases, as illustrated in Tab. 3 and Fig. 13.

Specimen	Pre-damage Level	Strengthening	Ultimate Deflection (mm)	Change vs Control
SS-Control	-	Without	17.57	-
SB-5-0	-	Without	19.20	+ 9.3%
SB-5-50	50 %	CFRP	13.64	- 22.4%
SB-5-60	60 %	CFRP	15.74	- 10.4%
SB-5-75	75 %	CFRP	13.12	- 25.3%
SB-6-0	-	Without	17.2	–2.3%
SB-6-50	50 %	CFRP	13.98	–20.6%
SB-6-60	60 %	CFRP	19.72	+12.0%
SB-6-75	75 %	CFRP	14.59	–17.1%

Table 3: Deflection at ultimate load.

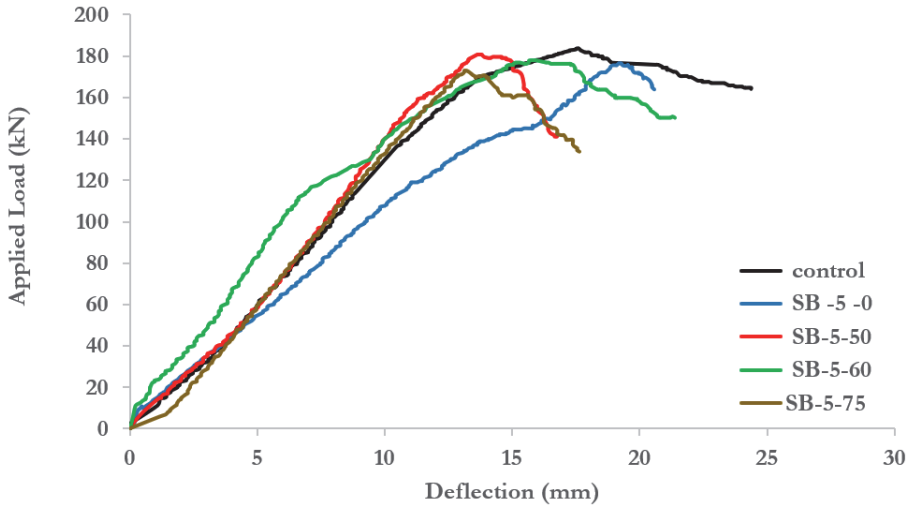

Figure 13: Load-deflection curve for specimens 50 mm.

The load-deflection curve demonstrates the impact of 60 mm cavities on the structure and the efficacy of the CFRP reinforcement at each of the preload levels employed. The Group 2 slabs exhibited a distinct behavior from the SS-Control slabs, attaining maximum strength and maximum displacement at the midpoint. The SB-6-0 specimen was loaded to approximately 86.5% of the control capacity, suggesting that the presence of bubble cavities led to a reduction in strength. Simultaneously, its deflection at failure was 2.3% lower than the other specimen's, suggesting that it was more effective in resisting bending. SB-6-50, which was equipped with 50% preload and CFRP, attained a load 93.7% greater than the control specimen.

Additionally, its deflection was only approximately 20.6% lower than the control specimen's. The final specimen was capable of withstanding nearly the entire peak load; however, it exhibited a partial increase in strength and flexed more than the control specimen. This illustrates that CFRP's resistance to deformation decreased as it approached failure. The deflection of SB-6-75 was 17% lower than that of SB-6-0, even though it retained only approximately 82.5% of the control load. This indicates that CFRP increases its strength despite a decrease in strength. The bubble sheets (SB-6-50) that were moderately damaged were substantially enhanced by CFRP re-molding, as evidenced by these graphs. The extent of injury increased prior to performance testing, resulting in decreased performance levels. CFRP could reduce deflection and slow brittle fractures with only 75% of the preload completed. Consequently, the structural behavior was influenced by both the applied preload intensity and the bubble dimensions, as illustrated in Tab. 3 and Fig. 14, and the strength enhancements from CFRP in Group 2 were not substantial.

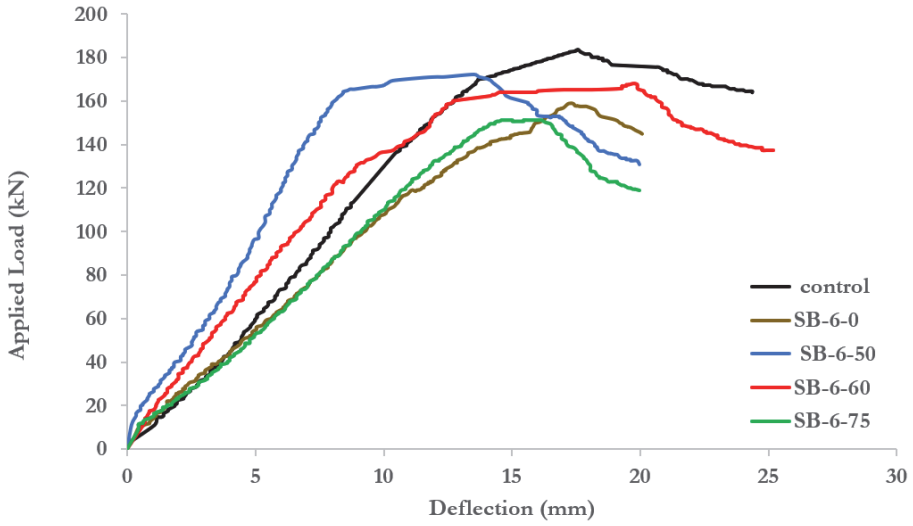

Figure 14: Load-deflection curve for specimens 60 mm.

COMPARATIVE ANALYSIS WITH EXISTING LITERATURE

The rehabilitation outcomes observed in this study are consistent with and expand upon the findings of previous research on CFRP-strengthened concrete elements. 98.5% of the solid slab's load capacity was recovered by the 50 mm void slabs preloaded to 50% and retrofitted with CFRP. This recovery rate exceeds the 90–92% recovery reported by Aborgheef and Abdulridha (2025) [9] for similarly pre-damaged corbels. The recovery rate for 60 mm void slabs decreased to 82.5% at 75% preloading, which is consistent with Khadim and Abdulridha (2024) [8], who observed that the efficacy of CFRP was reduced beyond 70% damage. The benefit of full-surface CFRP application was underscored by the 22–25% deflection reductions in 50 mm slabs, which exceeded the 15–18% reported by Mashrei et al. (2019) [6]. The performance decline observed with larger voids is consistent with Ghamry et al. (2022) [2], underscoring the necessity to balance structural resilience and void size in the design of lightweight slabs.

CONCLUSIONS

The study's findings are as follows:

1. The final load-bearing capacity of the unreinforced bubble slabs demonstrated a natural reduction in capacity when contrasted with the solid slab (SS-Control) due to the presence of spaces. In particular, the 50 mm thick unreinforced bubble slab (SB-5-0) exhibited a 4.1 percent reduction in ultimate load-carrying capacity and a 9.3 percent increase in deflection. Conversely, the bubble slab (SB-6-0) experienced a significant drop of 13.5 percent in ultimate load-carrying capacity, as well as a 2.3 percent increase in deflection. This demonstrated the trade-off between structural efficacy and weight loss.

2. The extent of the void substantially impacts the efficiency of retrofitting and the structure's performance. Unreinforced bubble slabs with 50 mm voids maintained 96.2% of the solid slab's load capacity, while those with 60 mm voids achieved only 86.5%. This suggests that smaller voids (≤50 mm) are more suitable for design when potential damage and subsequent rehabilitation are anticipated. In order to ensure that the concrete cover, shear transfer capacity, and bond integrity are sufficient for prospective CFRP retrofitting, engineers should consider restricting the void diameter in new bubble deck constructions.
3. While CFRP retrofitting effectively restores strength and rigidity, its efficacy decreases as pre-damage increases. The application of CFRP technology restored up to 98.5% of the solid slab's load capacity in 50 mm void slabs that had been pre-damaged to 50%. Additionally, the deflection was reduced by 25%. Nevertheless, the recovery rate for 60 mm vacuum slabs decreased to 82.5% at 75% preloading. The most effective application of CFRP is prior to a severe fracture. In order to optimize rehabilitation efficiency and cost-effectiveness, structural assessments should prioritize early intervention when damage is restricted to 50–60% of the ultimate burden.
4. Debonding is the predominant failure mode, not shear or flexural yielding. Flexural fracture and CFRP-concrete interfacial debonding were the causes of failure for all CFRP-strengthened specimens, and no punching shear failures were observed. This emphasizes that the bond interface, rather than the concrete or steel, determines the system's ultimate performance. In order to delay debonding and improve ductility in practical applications, engineers should conduct appropriate surface preparation (e.g., mechanical grinding, surface roughness control) and evaluate edge anchorage systems (e.g., U-jackets, end covers).
5. Larger voids diminish the efficacy of CFRP in stiffness recovery. Although CFRP substantially reduced deflection in 50 mm void slabs (up to 25% lower than control), the SB-6-60 specimen exhibited a 12% increase in deflection despite strengthening, suggesting that stiffness recovery was compromised at higher damage levels. In slabs with larger voids (e.g., 60 mm), it is imperative to conduct additional serviceability tests following the retrofitting process. In order to satisfy deflection criteria, designers may need to integrate CFRP with other stiffening techniques (e.g., partial infill, additional top reinforcement).
6. All tested slabs surpassed the serviceability deflection limit (L/240 = 4.17 mm). Although CFRP enhanced rigidity, ultimate deflections continued to exceed the permissible limit under service loads. CFRP alone may not be sufficient to ensure serviceability in bubble deck slabs that are severely loaded or have a long span. In high-performance or sensitive applications, it is advisable to consider a hybrid approach that combines CFRP with prestressing or supplementary supports.
7. Smaller voids provide a more dependable and effective rehabilitation platform. The superior performance of 50 mm void slabs implies optimizing void size is equally important as the strengthening method. In order to guarantee both weight reduction and robustness for prospective retrofitting, designers should implement a balanced void size (≤50 mm) for new constructions that are susceptible to future damage (e.g., parking structures, industrial floors).

LIMITATIONS OF THE STUDY

Utilizing a single specimen for each test condition is the primary constraint of this experimental investigation. The statistical reliability of the observed trends is restricted by the fact that only one sample per configuration is tested due to the inherent variability in material properties and failure mechanisms of concrete structures, particularly under flexural and piercing shear stresses. At the same time, the results should be interpreted cautiously, particularly regarding the generalization of failure modes and quantitative performance metrics. Consistent casting procedures, standardized curing conditions, and precise instrumentation were implemented to reduce variability. In order to establish statistical significance, the observed enhancements in load capacity and deflection control, while promising, would be enhanced by validation with a larger sample size. The objective of future research should be to replicate the experimental program with multiple specimens per group to improve the robustness of the data and facilitate probabilistic analysis.

PRACTICAL IMPLICATION FOR DESIGNERS

When long-term durability, serviceability, and potential future rehabilitation are design priorities, a void diameter of 50 mm is recommended over 60 mm for new construction projects that intend to use bubble deck slabs. Although 60 mm voids provide a minor increase in weight savings, they significantly compromise structural

performance and restrict the efficacy of CFRP retrofitting. Designers should evaluate lacuna size not only as a geometric parameter, but also as a critical factor in the structure's repairability and damage tolerance.

FUTURE RESEARCH RECOMMENDATIONS

Based on the findings of this study, future research should focus on exploring hybrid strengthening techniques combining CFRP with other materials (e.g., GFRP or steel plates), as well as developing improved bonding agents to address the observed debonding failures at the CFRP–concrete interface. Investigations into long-term durability under environmental exposure, including temperature variations, moisture, and chemical attack, are essential to assess real-world performance. Further studies should examine the behavior of CFRP-strengthened corbels under cyclic and seismic loads to evaluate fatigue resistance and structural resilience. Alternative wrapping configurations, full-surface coverage, and anchorage systems should be explored to enhance efficiency. Enhanced nonlinear finite element modeling would support accurate prediction of failure mechanisms and optimize design strategies

REFERENCES

[1] Cunha, R., Vieira, C. and Amorim, D. (2021). Lumped Damage Mechanics as a Diagnosis Tool of Reinforced Concrete Structures in Service: Case Studies of a Former Bridge Arch and a Balcony Slab, Frattura ed Integrità Strutturale, 15(58), pp. 21–32. DOI: https://doi.org/10.3221/igf-esis.58.02.

[2] Ghamry, A., Esia, A. and Aboul-Nour, L. (2022). Structural Behavior of Lightweight and High Strength Layered Hollow Core Slabs, Frattura ed Integrità Strutturale, 17(63), pp. 134–152. DOI: https://doi.org/10.3221/igf-esis.63.13

[3] Harba, I. S. and Abdulridha, A. (2017). Finite Element Analysis of RC Tapered Beams under Cyclic Loading, Al-Nahrain Journal for Engineering Sciences, 20(2), pp. 378-396. https://nahje.com/ index.php/main/article/view/ 117.

[4] Abdulridha, A. J. (2024). Behavior of a Multi-Story Reinforced Concrete Structure with CFRP-Strengthened Columns at the Lower Story, Asian Journal of Civil Engineering, 25(4), pp. 3637-3654. DOI: https://doi.org/10.1007/s42107-024-01001-3.

[5] Abdulridha, A. J. (2023). Behavior of a Multi-Story Steel Structure with Eccentric X-Brace, Frattura Ed Integrità Strutturale, 17(66), pp. 273-296. DOI: https://doi.org/10.3221/igf-esis.66.17.

[6] Mashrei, M. A., Makki, J. S. and Sultan, A. A. (2019). Flexural Strengthening of Reinforced Concrete Beams Using Carbon Fiber Reinforced Polymer (CFRP) Sheets with Grooves, Latin American Journal of Solids and Structures, 16(4). DOI: https://doi.org/10.1590/1679-78255514.

[7] Ismael, B. H., Hama, S. M., Ali, Z. M., Aljumaily, M. M., Fayyadh, A. H. and AlOmar, M. K. (2025). Structural Behavior of Voided Fibrous Sustainable Ferrocement Slabs, Journal of Engineering, 2025(1). DOI: https://doi.org/10.1155/je/8870378.

[8] Khadim, M. and Abdulridha, A. (2024). Behavior of Reinforced Lightweight Concrete Slab with Initial Cracks. Frattura Ed Integrità Strutturale, 18(69), pp. 181–191. DOI: https://doi.org/10.3221/igf-esis.69.13.

[9] Aborgheef, S. and Abdulridha, A. J. (2025). Optimizing Different Damaged Reinforced Concrete Corbel Characteristics Utilizing CFRP Sheets, Fracture and Structural Integrity, 19(74), pp. 31–41. DOI: https://doi.org/10.3221/IGF-ESIS.74.03.

[10] Ranjitham, M. and Manjunath, N. V. (2018). Experimental and Numerical Investigation on Structural Behaviour of Bubble Deck Slab with Conventional Slab, International Journal of Trend in Scientific Research and Development, 2(3), pp. 2614-2617. DOI: https://doi.org/10.31142/ijtsrd11532.

[11] Anusha, M., Surendra, H., Vinod, B. and Bhavya, S. (2022). Modelling Using Finite Element Analysis in the Structural Behavior of Bubble Deck Slab, Materials Today Proceedings, 66, pp. 2397-2404. DOI: https://doi.org/10.1016/j.matpr.2022.06.337.

[12] Pardeshi, M., Mulla, S., Gawde, S., Gawari, T., Chavan, A., Raut, S. and Bhide, M. (2025). A Comparative Study of Post Tension Voided Slab, International Journal of Innovative Research in Engineering and Multidisciplinary Physical Sciences, 13(3). DOI: https://doi.org/10.37082/ijirmps. v13.i3.232471.

[13] Hegab, A. A., Kassem, M. E. and Mabrouk, R. T. S. (2025). Flexural Behaviour of Prestressed Post-Tension Voided Biaxial Slab under Uniformly Distributed Load, Civil Engineering Journal, 11(5), pp. 1870-1890. DOI: https://doi.org/10.28991/cej-2025-011-05-09.

[14] Zarzour, A. M., Almutairi, A. L., Ahmed, S. N., Hamid, W. K. and Abdalla, H. A. (2025). Repairing of RC Beams with Openings Subjected to Torsion using CFRP, Civil and Environmental Engineering. DOI: https://doi.org/10.2478/cee-2025-0047.
[15] Elkhatib, L., Khatib, J., Fırat, S., Hassan, H. E. Elkordi, A. (2024). Rehabilitation of Concrete Structures - A Review, Gazi University Journal of Science. DOI: https://doi.org/10.35378/gujs.1503207.
[16] Elhadi, K. M., Abdellatif, S., Raza, A. and Arshad, M. (2023). Efficiency of Rapid Repairing for Composites and Structural Fibre-Reinforced Plastic Waste Aggregate Concrete Members, Structures, 56, 105061. DOI: https://doi.org/10.1016/j.istruc.2023.105061.
[17] Thanh, C. L., Minh, H. and Sang-To, T. (2021). A Nonlinear Concrete Damaged Plasticity Model for Simulation Reinforced Concrete Structures Using ABAQUS, Frattura ed Integrità Strutturale, 16(59), pp. 232–242. DOI: https://doi.org/10.3221/igf-esis.59.17.
[18] Humam, A. M. (2018). Experimental Study on the Strength and Behavior of One-Way Bubbled Reinforced Concrete Slabs, Journal of Structural Engineering, 144(5), 04018003.
[19] Lee, C. H., Mansouri, I., Kim, E., Ryu, J. and Woo, W. T. (2019). Experimental Analysis of One-Way Composite Steel Deck Slabs Voided by Circular Paper Tubes: Shear Strength and Moment–Shear Interaction, Engineering Structures, 182, pp. 227–240.
[20] ASTM International. (2022). ASTM A1064/A1064M-22 Standard Specification for Carbon-Steel Wire and Welded Wire Reinforcement, Plain and Deformed, for Concrete. DOI: https://doi.org/10.1520/A1064_A1064M-22.
[21] ASTM International. (2024). ASTM C39/C39M-24: Standard Test Method for Compressive Strength of Cylindrical Concrete Specimens. DOI: https://doi.org/10.1520/C0039_C0039M-24.
[22] Committee, A. (2017). ACI 440. 2R-17 Guide for The Design and Construction of Externally Bonded FRP Systems for Strengthening Concrete Structures.
[23] ASTM International. (2021). ASTM D7234-21: Standard Test Method for Pull-Off Adhesion Strength of Coatings on Concrete Using Portable Pull-Off Adhesion Testers. DOI: https://doi.org/10.1520/D7234-21.